SEARCH FOR EXCITED MUONS AT THE FUTURE SPPC-BASED MUON–PROTON COLLIDERS*

A. Caliskan

Gümüşhane University, Faculty of Engineering and Natural Sciences
Department of Physics Engineering, 29100 Gümüşhane, Turkey

(Received July 10, 2018; accepted May 28, 2019)

We have investigated the production potential of the spin-1/2 excited muons, predicted by preonic models, at the four SPPC (Super Proton–Proton Collider)-based muon–proton colliders in different center-of-mass energies. For the signal process $\mu p \to \mu^\star X \to \mu\gamma X$, the production cross section and the decay width values of the excited muons have been calculated. The pseudorapidity and transverse momentum distributions of muons and photons in the final state have been obtained in order to choose the kinematical cuts best suited for enhancing the statistical signal of the excited muon signature. By applying these cuts, we report the discovery, observation and exclusion mass limits of the excited muons for two compositeness scale values, which are an energy level at which new interactions are expected to occur. It is shown that the discovery limits on the excited muons in the case the compositeness scale equals 100 TeV are 2.7, 3.9, 3.1 and 6.7 TeV for center-of-mass energies of 10.3, 14.2, 14.6 and 20.2 TeV, respectively.

DOI:10.5506/APhysPolB.50.1409

1. Introduction

In the particle physics, all matter and antimatter consist of two kinds of elementary particles: leptons and quarks. The electromagnetic, weak and strong forces among these particles are described very well by the Standard Model (SM). Despite all this success, there are some issues which have not entirely been solved by the SM, such as large number of free parameters, CP violation, fermion mass generation and fermion mixing. A lot of alternative theories beyond the SM (BSM), such as Technicolour [1, 2], Grand Unified Models [3, 4], Supersymmetry [5], Compositeness [6] have been proposed to solve these issues.

Compositeness is one of the BSM scenarios that better explains the proliferation of elementary particles and quark–lepton symmetry, introducing new fundamental constituents, called preons, out of which the leptons, quarks and their antiparticles are built. Countless preonic models have been suggested so far, by the particle physicists, and some new types of particles are introduced in the framework of these models, such as excited fermions, leptoquarks, leptogluons and color sextet quarks. The simplest preon model, for example, is the Harari–Shupe model [7, 8] in which leptons and quarks are bound states of two elementary, massless spin-$1/2$ preons, called T- and V-rishons, which carry both color and hypercolor charges. New hypercolor interactions among the fermions should exist at the energy scale (Λ) that binds the preons together. This energy scale is an important parameter that is commonly used in all composite models, and called the compositeness scale, Λ. Quarks and leptons are composed of three preons for this model, and they are hypercolor singlets that can be observed at lower energies than the Λ. In this energy region, the all preons become confined in composite particles and cannot be observed directly.

If the SM fermions are composite, they must have the excited states as a result of the compositeness. Therefore, the excited fermions could be considered as the excited state of the SM fermions that are in ground state and should be observed experimentally. The excited fermions are predicted by the preonic models. They were firstly proposed in 1977, and studied in detail in the following years [9–12]. The excited leptons and quarks can have spin-$1/2$ and spin-$3/2$ states, and it is expected that their masses are heavier than those of the SM fermion. In the present study, we are interested in the excited muons with spin-$1/2$ as a continuation of our recent works about the excited leptons [13]. There are also considerable phenomenological studies on production and decay of the excited quarks and leptons via the gauge and contact interactions [14–23].

Even though no signals for the excited leptons have been found in the experimental studies at the LEP [24], HERA [25], Tevatron [26], ATLAS [27] and CMS [28] experiments, the more powerful accelerators that will be established in the future are hopeful for their discovery. A possible discovery of the excited leptons will provide a direct evidence of the excited lepton compositeness. The recent experimental mass limits on the excited muons for pair and single production are provided by the OPAL [29] and CMS collaborations [30], respectively. Exclusion limits of the excited muons are $m_{\mu^\star} > 103.2$ GeV for $e^+e^- \to \mu^\star\mu^\star$ and $m_{\mu^\star} > 3800$ GeV for $pp \to \mu\mu^\star X$, assuming the coupling parameter of $f = f' = 1$ and the energy scale of $\Lambda = m_{\mu^\star}$.

Except for the gauge interactions, one of the production mechanisms of the excited leptons is four-fermion contact interactions. The contact interactions provide important contributions to excited lepton and quark production. It is known that the contact interactions are dominant at the proton–proton (antiproton) collisions. In recent studies, the production cross sections of the heavy leptons for both mechanisms were compared at the LHC energies, and it was clearly shown that contact interactions were dominant (see Refs. [20, 21]). In addition, the graphs of the decay width of the excited leptons belonging to both mechanisms were drawn and the results were compared. It has been shown that the most contribution to the width of the decay of the excited leptons again comes from the contact interactions. Therefore, for the production and decay of the excited leptons, the contact interaction mechanism was used in these studies. In this paper, we concentrated on the gauge interaction mechanism for a future muon–proton collider. Besides, we have planned to investigate the excited muon production via contact interactions in the framework of next study, as a continuation of the current work.

We have investigated the excited muon production at the four different center-of-mass energies of SPPC-based muon–proton colliders. We present the SPPC-based muon–proton colliders and their main parameters in Section 2, the excited muon interaction Lagrangian, its decay widths and the cross sections in Section 3, and the signal-background analysis in Section 4. Finally, we have reported all results in the last section.

2. The SPPC-based muon–proton colliders

The discovery of the Higgs particle with a mass of 125 GeV at the Large Hadron Collider (LHC) in 2012 [31, 32] confirmed the electroweak symmetry breaking mechanism of the SM. With this discovery, the particle physics has reached the Higgs era, but it is not known whether the observed Higgs particle is the fundamental scalar. To study the properties of the Higgs boson in detail and understand its true nature, the world of high-energy physics community has started to investigate the feasibility of a Higgs factory. It is known that the hadron colliders like the LHC have the highest center-of-mass energy values, so they are called the discovery machines, while the lepton and lepton–hadron colliders provide the smaller ones, and are called the precision machines. Recently, various future collider projects have begun to be designed by the accelerator physicists such as the ILC (International Linear Collider) [33], LHeC (Large Hadron Electron Collider) [34] and CLIC (Compact Linear Collider) [35] to search primarily the Higgs physics.

In the post-LHC era, the most important collider project in Europe is the International Future Circular Collider (FCC) [36] that is a circular proton–proton collider with a center-of-mass energy of 100 TeV. It has been launched in 2010–2013 at CERN, and supported by the European Union within the Horizon 2020 Framework for Research and Innovation. The main purpose of this project is to establish a 100 TeV energy-frontier hadron collider (FCC-hh) to be allocated in a new 80–100 km tunnel at CERN. As an intermediate step of the FCC project, it also involves a high-luminosity lepton collider (FCC-ee or TLEP [37]) with a center-of-mass energy of 90–400 GeV, to be installed in the same tunnel, as that of a lepton–hadron collider option (FCC-he). The FCC will give us the opportunity to explore the properties of Higgs boson, new interactions beyond the SM, top quark *etc.*, at the highest energies. The CDR (Conceptual Design Report) of the FCC was written as four volumes [38–41].

In parallel with the developments related to the FCC project in Europe, the Chinese physicists have initiated the design study of a two-stage circular collider project in 2012, called the CEPC-SPPC. The first stage of the project is a circular electron–positron collider (CEPC) with a center-of-mass energy of 240 GeV, to search the properties of Higgs particle. After completing its mission, the CEPC will be upgraded to the second stage that is a Super Proton–Proton Collider (SPPC) with a center-of-mass energy of more than 70 TeV, aiming at the search of the BSM physics. The Preliminary Conceptual Design Report (Pre-CDR) of the CEPC-SPPC project has been completed by the CEPC-SPPC study group in 2015 [42]. By using the same tunnel as the CEPC that is 54.7 km in circumference, center-of-mass energy of about 70 TeV will be tried to be reached. However, larger circumference options for the SPPC collider are also being considered. Table I presents the main parameters for the all design options of the SPPC collider [43].

If a TeV energy muon collider is installed tangentially to the SPPC, a muon–proton collider at the high center-of-mass energy can be obtained. Taking into account the energy values of 0.75 and 1.5 TeV for muon beam, and design options of 35.6 and 68 TeV of the SPPC, four muon–proton collider options have been recently proposed [44]. The excited muon production potential at these four muon–proton colliders have been analyzed in this paper, and the basic parameters of the machines are shown in Table II, where E_μ and E_p are energy of the muon and proton beam, respectively, $\sqrt{s}$ is the center-of-mass energy of collider, L_{int} is the integrated luminosity of the collider, ξ_μ and ξ_p denote beam–beam tune shift of the muon and proton beam, respectively. Since a suitable detector is not yet designed for the SPPC-based muon collider, a fast-simulation of the reconstructing of the final-state particles is not done. Thus, this analysis is at the parton level.

TABLE I

The main parameters of proton beams in the SPPC collider for the various design options.

Parameters	Option-1 (Pre-CDR)	Option-2	Option-3	Option-4	Option-5
Beam energy [TeV]	35.6	35	50	68	50
Circumference [km]	54.7	54.7	100	100	78
Dipole field [T]	20	19.69	14.73	20.03	19.49
Peak luminosity [$\times 10^{35}$cm^{-2}s^{-1}]	1.1	1.2	1.52	10.2	1.52
Particle per bunch [10^{11}]	2	2	2	2	2
Norm. transverse emittance [μm]	4.1	3.72	3.65	3.05	3.36
Bunch number per beam	5835	5835	10667	10667	8320
Bunch length [mm]	75.5	56.5	65	15.8	70.6
Bunch spacing [ns]	25	25	25	25	25

TABLE II

The main parameters of the SPPC-based muon–proton colliders.

Colliders	E_μ [TeV]	E_p [TeV]	$\sqrt{s}$ [fb^{-1}]	L_{int}	ξ_μ	ξ_p
μ750-SPPC1	0.75	35.6	10.33	5.5	8.7×10^{-3}	6×10^{-2}
μ750-SPPC2	0.75	68	14.28	12.5	8.7×10^{-3}	8×10^{-2}
μ1500-SPPC1	1.5	35.6	14.61	4.9	8.7×10^{-3}	6×10^{-2}
μ1500-SPPC2	1.5	68	20.2	42.8	8.7×10^{-3}	8×10^{-2}

3. The excited muons

The interactions of an excited lepton with ordinary leptons are of magnetic-transition-type when the production or decay is via gauge interaction, and the effective Lagrangian that describes the interaction between a spin-1/2 excited lepton, the SM lepton and a gauge boson is given as [45–48]

$$L = \frac{1}{2\Lambda}\overline{l_R^\star}\sigma^{\mu\nu}\left[fg\frac{\vec{\tau}}{2}\cdot\vec{W}_{\mu\nu} + f'g'\frac{Y}{2}B_{\mu\nu}\right]l_L + \text{h.c.}\,, \tag{1}$$

where l and $l^\star$ represent the SM lepton and the excited lepton, respectively, Λ is the new physics scale, $\vec{W}_{\mu\nu}$ and $B_{\mu\nu}$ are the field strength tensors,

g and g' are the SM gauge couplings of SU(2) and U(1), f and f' are the new scaling factors for the gauge couplings, Y is hypercharge, $\sigma^{\mu\nu} = i(\gamma^\mu\gamma^\nu - \gamma^\nu\gamma^\mu)/2$, where γ^μ are the Dirac matrices, and $\vec{\tau}$ denotes the Pauli matrices.

The excited muons can decay into three channels that are γ-channel ($\mu^\star \to \mu\gamma$), Z-channel ($\mu^\star \to \mu Z$) and W-channel ($\mu^\star \to \mu W$). The decay widths of the excited muons for the gauge interactions are given by the following formula:

$$\Gamma(l^\star \to lV) = \frac{\alpha m^{\star 3}}{4\Lambda^2} f_V^2 \left(1 - \frac{m_V^2}{m^{\star 2}}\right)^2 \left(1 + \frac{m_V^2}{2m^{\star 2}}\right), \tag{2}$$

where $m^\star$ is the mass of the excited electron, m_V is the mass of the gauge boson, f_V is the new electroweak coupling parameter corresponding to the gauge boson V, where $V = W, Z, \gamma$, and $f_\gamma = -(f+f')/2$, $f_Z = (-f\cot\theta_{\mathrm{W}} + f\tan\theta_{\mathrm{W}})/2$, $f_W = (f/\sqrt{2}\sin\theta_{\mathrm{W}})$, where θ_{W} is the weak mixing angle, and α is the electromagnetic coupling constant.

For the numerical calculations, we implemented the excited muon interaction vertices into the high-energy simulation programme of CALCHEP [49]. Figure 1 shows the total decay widths of the excited muons for energy scales $\Lambda = m_{\mu^\star}$ and $\Lambda = 100$ TeV. The total cross sections of the excited muons produced at the four different muon–proton colliders, which are μ750-SPPC1, μ750-SPPC2, μ750-SPPC2, μ1500-SPPC1, μ1500-SPPC2, are shown in Fig. 2, using the program CALCHEP with the CTEQ6L parton distribution functions [50]. It is unambiguously seen from the figure that the excited muons have sufficiently high cross sections for both energy scales.

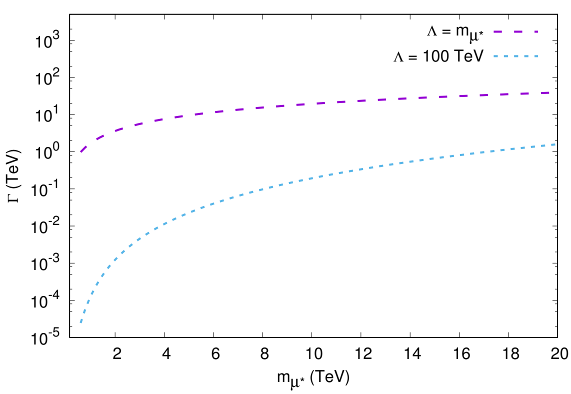

Fig. 1. The total decay widths of the excited muons for $\Lambda = m_{\mu^\star}$ and $\Lambda = 100$ TeV, assuming $f = f' = 1$.

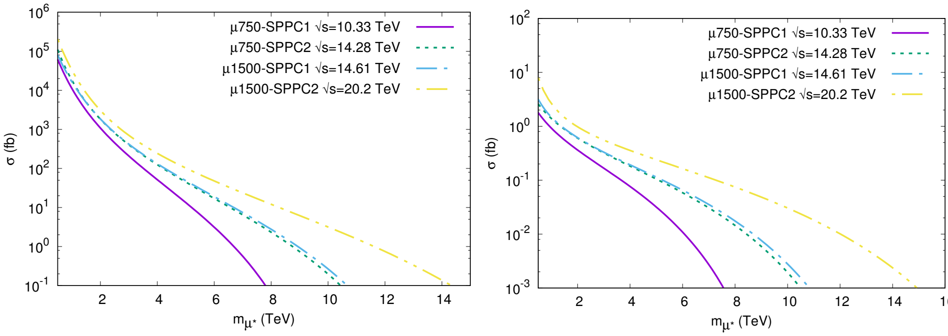

Fig. 2. The total cross-section values of the excited muons with respect to its mass at the various muon–proton colliders for $\Lambda = m_{\mu^\star}$ (left) and $\Lambda = 100$ TeV (right), assuming $f = f' = 1$.

4. Signal and background analysis

The SPPC-based muon–proton colliders will allow us to search for excited muons via the process $\mu p \to \mu^\star X$ with subsequent decays of the excited muons into a muon and photon. Therefore, our signal and background process is $\mu p \to \mu, \gamma, j$ through γ and Z exchange, where j represents jets which are composed of quarks $(u, \bar{u}, d, \bar{d}, c, \bar{c}, s, \bar{s}, b, \bar{b})$, while the subprocesses are $\mu q(\bar{q}) \to \mu\gamma q(\bar{q})$, where q denotes quarks (u, d, s, c, b) and $\bar{q}$ denotes anti-quarks $(\bar{u}, \bar{d}, \bar{c}, \bar{s}, \bar{b})$. The Feynman diagrams of signal and background processes are shown in Fig. 3 and Fig. 4, respectively.

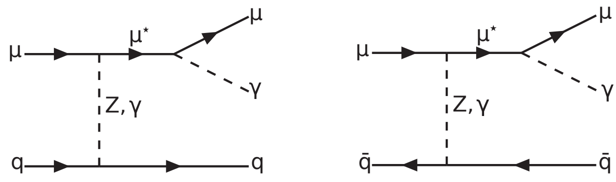

Fig. 3. Leading-order Feynman diagrams of the signal process.

In order to separate the excited muon signals from the background, we have applied pre-selection cuts to the transverse momentum of the muon, photon and jet in the final state, as $p_{\mathrm{T}}^{\mu,\gamma,j} > 20$ GeV. The SM cross-section values after the application of these prime cuts have been obtained as $\sigma_{\mathrm{B}} = 73.15$ pb for μ750-SPPC1, $\sigma_{\mathrm{B}} = 82.11$ pb for μ750-SPPC2, $\sigma_{\mathrm{B}} = 84.65$ pb for μ1500-SPPC1, $\sigma_{\mathrm{B}} = 126.84$ pb for μ1500-SPPC2 collider. To assign the kinematical cuts best suited for the discovery of the excited muons, we have to look at the transverse momentum (p_{T}) and pseudorapidity (η) distributions of the final-state particles for both the signal and background.

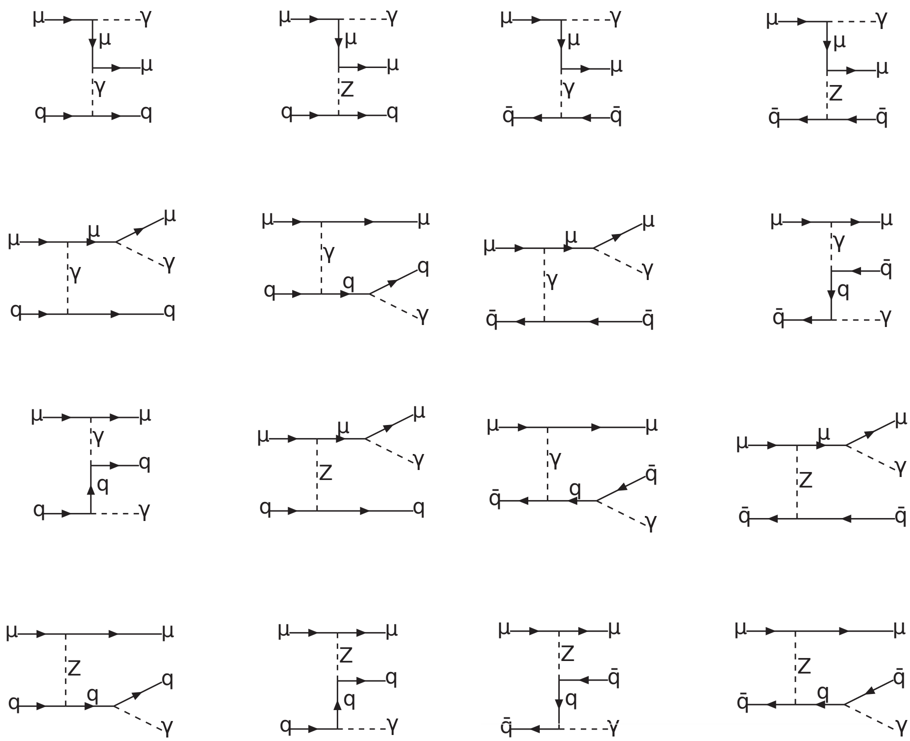

Fig. 4. Leading-order Feynmann diagrams of the background process.

The normalized η and p_{T} distributions of the final-state muons and normalized η distributions of the final-state photons are shown in Fig. 5 for μ750-SPPC1, Fig. 6 for μ750-SPPC2, Fig. 7 for μ1500-SPPC1 and Fig. 8 for μ1500-SPPC2, for both the signal and background. Since the p_{T} distributions of the muons are the same as those of the photons for all colliders, we

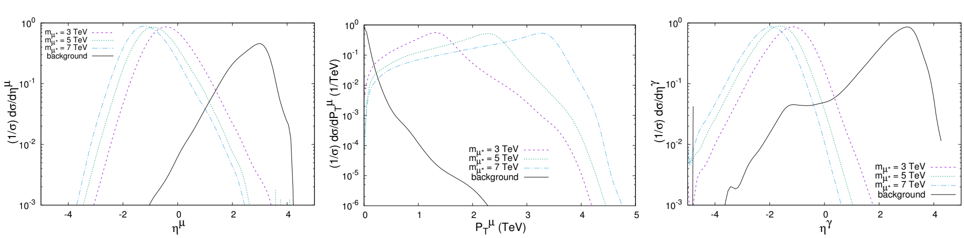

Fig. 5. The normalized pseudorapidity (left) and transverse momentum (middle) distributions of the final-state muons and the normalized pseudorapidity distributions of the final-state photons (right) at the μ750-SPPC1 collider, for $f = f' = 1$ and $\Lambda = m_{\mu^\star}$.

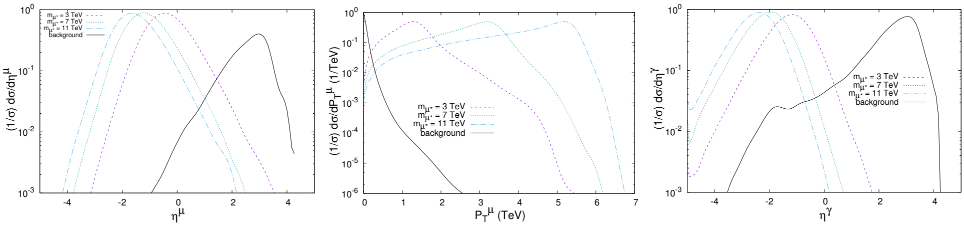

Fig. 6. The normalized pseudorapidity (left) and transverse momentum (middle) distributions of the final-state muons and the normalized pseudorapidity distributions of the final-state photons (right) at the μ750-SPPC2 collider, for $f = f' = 1$ and $\Lambda = m_{\mu^\star}$.

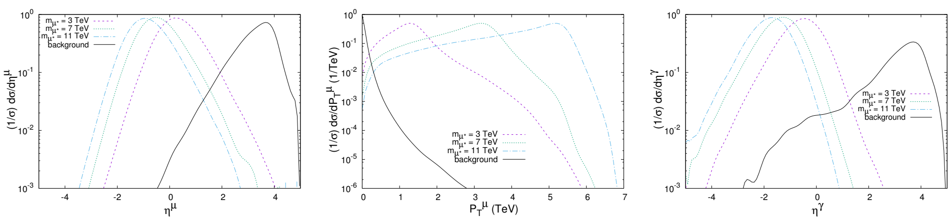

Fig. 7. The normalized pseudorapidity (left) and transverse momentum (middle) distributions of the final-state muons and the normalized pseudorapidity distributions of the final-state photons (right) at the μ1500-SPPC1 collider, for $f = f' = 1$ and $\Lambda = m_{\mu^\star}$.

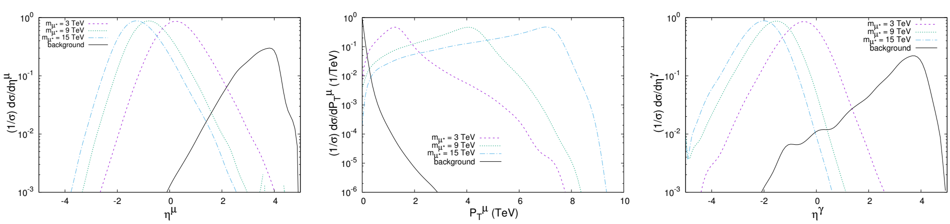

Fig. 8. The normalized pseudorapidity (left) and transverse momentum (middle) distributions of the final-state muons and the normalized pseudorapidity distributions of the final-state photons (right) at the μ1500-SPPC2 collider, for $f = f' = 1$ and $\Lambda = m_{\mu^\star}$.

have only shown the ones of the muons in these figures. The η distributions of the both particles in the final state are generally peaked in the negative region for all colliders. Since the pseudorapidity is mathematically defined as $\eta = -\ln\tan(\theta/2)$, where θ is the polar angle, the muon and photon are of backward, so we can say that the excited muons are mostly produced in the backward direction. In addition, since the energy of the muon beam was less than the one of the proton beam, the η distributions were shifted to the muon beam side, and these distributions showed an asymmetric behavior.

It is seen that the signal and background curves in the η and p_{T} distributions are separated from each other for both particles in the final state. Thus, we have easily chosen optimal regions, where we cut off most of the background but at the same time keep the signal almost unchanged, by applying a cut on both η and p_{T} distributions of the final-state particles. The determined discovery cuts for all colliders are reported in Table III.

TABLE III

The discovery cuts for the excited muons.

Colliders	p_{T}^{μ}	p_{T}^{γ}	η^{μ}	η^{γ}
μ750-SPPC1	$p_{\mathrm{T}}^{\mu} > 500$ GeV	$p_{\mathrm{T}}^{\gamma} > 500$ GeV	$-5 < \eta^{\mu} < 1$	$-4.8 < \eta^{\gamma} < 0$
μ750-SPPC2	$p_{\mathrm{T}}^{\mu} > 600$ GeV	$p_{\mathrm{T}}^{\gamma} > 500$ GeV	$-5 < \eta^{\mu} < 1.5$	$-5 < \eta^{\gamma} < 0.5$
μ1500-SPPC1	$p_{\mathrm{T}}^{\mu} > 600$ GeV	$p_{\mathrm{T}}^{\gamma} > 500$ GeV	$-5 < \eta^{\mu} < 2$	$-5 < \eta^{\gamma} < 1.5$
μ1500-SPPC2	$p_{\mathrm{T}}^{\mu} > 750$ GeV	$p_{\mathrm{T}}^{\gamma} > 750$ GeV	$-5 < \eta^{\mu} < 2.2$	$-5 < \eta^{\gamma} < 1.4$

The invariant mass distributions of the $\mu\gamma$ system after the application of all discovery cuts are presented in Fig. 9. As is clearly seen from this figure, the separation of the signal from the background became better.

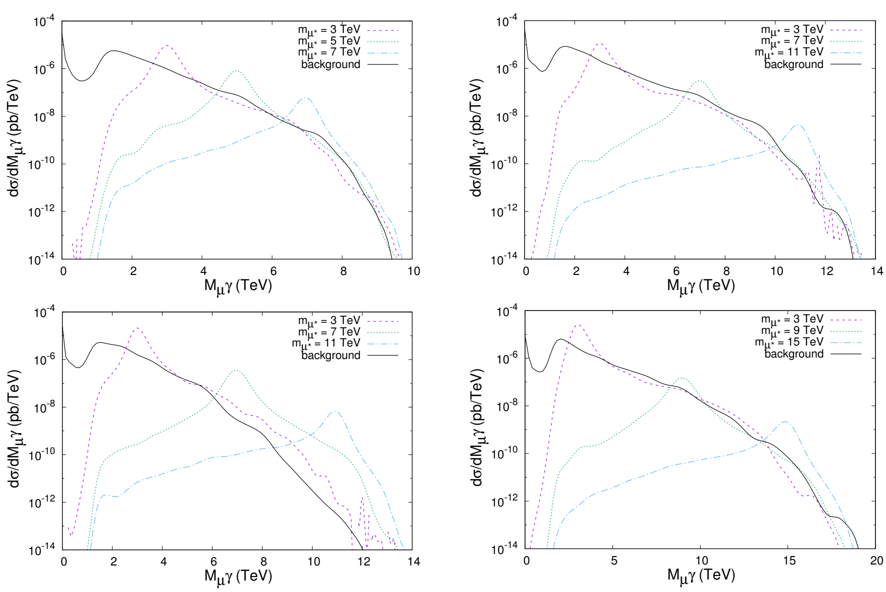

Fig. 9. The invariant mass distributions of the excited muon signal and the corresponding background for $\Lambda = m_{\mu^{\star}}$ and $f = f' = 1$ at the colliders of μ750-SPPC1 (top left), μ750-SPPC2 (top right), μ1500-SPPC1 (bottom left) and μ1500-SPPC2 (bottom right).

To extract the excited muon signal from the background, in addition to the discovery cuts, we have imposed a cut on the $\mu\gamma$-invariant mass as $m_{\mu^\star} - 2\Gamma_{\mu^\star} < m_{\mu\gamma} < m_{\mu^\star} + 2\Gamma_{\mu^\star}$, where Γ denotes the decay width of the excited muon. Table IV shows the event numbers before/after all cuts, and corresponding efficiencies for both signal and background.

TABLE IV

The efficiencies of the standard model background and of our signature after the application of all kinematical cuts.

Colliders			Event number before cut	Event number after cut	Efficiency (ϵ)
μ750-SPPC1	background		469755	74.91	0.000159
	signal [GeV]	3000	354.2	176.44	0.4981
		5000	19.47	10.02	0.5146
		7000	0.96	0.42	0.4390
μ750-SPPC2	background		1815000	226.75	0.000124
	signal [GeV]	3000	2031.25	1141	0.5617
		7000	22.06	9.63	0.4365
		11000	0.16	0.05	0.3125
μ1500-SPPC1	background		662970	124.41	0.000187
	signal [GeV]	3000	1962.45	809.97	0.4127
		7000	10.51	4.64	0.4414
		11000	0.09	0.02	0.2959
μ1500-SPPC2	background		7049160	735.30	0.000104
	signal [GeV]	3000	41725.72	32532.28	0.7796
		9000	71.90	27.13	0.3773
		15000	1.27	0.13	0.1023

For statistical significance (SS) of the excited muon signal, we have used the following formula [51]:

$$\mathrm{SS} = \frac{|\sigma_{\mathrm{S+B}} - \sigma_{\mathrm{B}}|}{\sqrt{\sigma_{\mathrm{B}}}} \sqrt{L_{\mathrm{int}}}\,, \tag{3}$$

where $\sigma_{\mathrm{S+B}}$ denotes the cross section from the signal and the background, σ_{B} denotes the background cross section, and L_{int} is the integrated luminosity of the collider. Taking into account the discovery criterion SS ≥ 5, mass limits on the excited muon have been calculated as 6600, 8700, 7200, 11100 GeV for the colliders of μ750-SPPC1, μ750-SPPC2, μ1500-SPPC1, μ1500-SPPC2, respectively, assuming $f = f' = 1$ and $\Lambda = m_{\mu^\star}$. For the $\Lambda = 100$ TeV and the same criteria, excited muon mass limits are 2780, 3900, 3100 and 6700 GeV, respectively.

5. Conclusion

We have studied the production of the excited muon at the SPPC-based muon–proton colliders. This work has shown us that these colliders have a great research potential for the excited muon searches. We give a realistic estimate for the excited muon signal and the corresponding background at the SPPC-based muon–proton colliders, namely the μ750-SPPC1 ($\sqrt{s} = 10.33$ TeV), the μ750-SPPC2 ($\sqrt{s} = 14.28$ TeV), the μ1500-SPPC1 ($\sqrt{s} = 14.61$ TeV) and the μ1500-SPPC2 ($\sqrt{s} = 20.2$ TeV). In the simulations performed to obtain the pseudorapidity and transverse momentum distributions, it is assumed that the energy scale is $\Lambda = m_{\mu^\star}$ and the coupling parameter is $f = f' = 1$. The mass limits for exclusion, observation, and discovery of the excited muons at the four colliders are reported in Table V, for both $\Lambda = m_{\mu^\star}$ and $\Lambda = 100$ TeV. As a result, the future SPPC-based muon–proton colliders offer the possibility to investigate the excited muon in a very wide range of mass.

TABLE V

The mass limits for the exclusion (2σ), observation (3σ), and discovery (5σ) of the excited muons at the SPPC-based μp colliders assuming the coupling $f = f' = 1$.

Colliders	L_{int} [fb^{-1}]	Λ	2σ [GeV]	3σ [GeV]	5σ [GeV]
μ750-SPPC1	5.5	$m_{\mu^\star}$	7400	7000	6600
		100 TeV	4010	3750	2780
μ750-SPPC2	12.5	$m_{\mu^\star}$	10600	9200	8700
		100 TeV	6500	5000	3900
μ1500-SPPC1	4.9	$m_{\mu^\star}$	9000	8600	7200
		100 TeV	5000	4400	3100
μ1500-SPPC2	42.8	$m_{\mu^\star}$	13200	12600	11100
		100 TeV	8700	8100	6700

I would like to thank A. Ozansoy for model file support. This work has been supported by the Scientific and Technological Research Council of Turkey (TUBITAK) under grant No. 114F337.

REFERENCES

[1] S. Weinberg, *Phys. Rev. D* **13**, 974 (1976).

[2] L. Susskind, *Phys. Rev. D* **20**, 2619 (1979).

[3] H. Georgi, S.L. Glashow, *Phys. Rev. Lett.* **32**, 438 (1974).

[4] J.C. Pati, A. Salam, *Phys. Rev. D* **10**, 275 (1974).

[5] Y.A. Golfand, E.P. Likhttman, *JETP Lett.* **13**, 323 (1971).

[6] I.A. D'Souza, C.S. Kalman, *Preons: Models of Leptons, Quarks and Gauge Bosons as Composite Objects*, World Scientific Publishing, 1992.

[7] H. Harari, *Phys. Lett. B* **86**, 83 (1979).

[8] M.A. Shupe, *Phys. Lett. B* **86**, 87 (1979).

[9] H. Terazawa, Y. Chikashige, K. Akama, *Phys. Rev. D* **15**, 480 (1977).

[10] H. Terazawa, *Phys. Rev. D* **22**, 184 (1980).

[11] H. Terazawa, M. Yasue, K. Akama, M. Hayashi, *Phys. Lett. B* **112**, 387 (1982).

[12] H. Terazawa, *Phys. Lett. B* **133**, 57 (1983).

[13] A. Caliskan, *Adv. High Energy Phys.* **2017**, 4726050 (2017).

[14] Y.O. Günaydın, M. Sahin, S. Sultansoy, *Acta Phys. Pol. B* **49**, 1763 (2018).

[15] O. Panella *et al.*, *Phys. Rev. D* **96**, 075034 (2017).

[16] A. Ozansoy, A.A. Billur, *Phys. Rev. D* **86**, 055008 (2012).

[17] M. Köksal, *Int. J. Mod. Phys. A* **29**, 1450138 (2014).

[18] A. Ozansoy, V. Ari, V. Cetinkaya, *Adv. High Energy Phys.* **2016**, 1739027 (2016).

[19] S. Biondini *et al.*, *Phys. Rev. D* **85**, 095018 (2012).

[20] R. Leonardi, O. Panella, L. Fano, *Phys. Rev. D* **90**, 035001 (2014).

[21] R. Leonardi *et al.*, *Eur. Phys. J. C* **76**, 593 (2016).

[22] S. Biondini, O. Panella, *Eur. Phys. J. C* **77**, 644 (2017).

[23] CMS Collaboration, *Phys. Lett. B* **775**, 315 (2017).

[24] L3 Collaboration, *Phys. Lett. B* **568**, 1 (2003).

[25] H1 Collaboration, *Phys. Lett. B* **666**, 131 (2008).

[26] D0 Collaboration, *Phys. Rev. D* **77**, 091102 (2008).

[27] ATLAS Collaboration, *New J. Phys.* **15**, 093011 (2013).

[28] CMS Collaboration, *J. High Energy Phys.* **1603**, 125 (2016).

[29] M. Tanabashi *et al.* [Particle Data Group], *Phys. Rev. D* **98**, 030001 (2018).

[30] CMS Collaboration, *J. High Energy Phys.* **1904**, 015 (2019) [`arXiv:1811.03052 [hep-ex]`].

[31] ATLAS Collaboration, *Phys. Lett. B* **716**, 1 (2012).

[32] CMS Collaboration, *Phys. Lett. B* **716**, 30 (2012).

[33] C. Adolphsen *et al.*, `arXiv:1306.6328 [physics.acc-ph]`.

[34] LHeC Project Web Page: http://lhec.web.cern.ch

[35] CLIC Collaboration, The CLIC Programme: Towards a Staged e^+e^-linear Collider Exploring the Terascale, CLIC Conceptual Design Report, CERN-2012-005, CERN, Geneva 2012.

[36] FCC Project Web Page: https://fcc.web.cern.ch

[37] TLEP Project Web Page: https://tlep.web.cern.ch

[38] FCC Collaboration, Future Circular Collider Study Volume 1: Physics Opportunities, Conceptual Design Report, edited by M. Mangano *et al.*, CERN Accelerator Reports, CERN-ACC-2018-0056, submitted to *Eur. Phys. J. C*, Geneva 2018.

[39] FCC Collaboration, Future Circular Collider Study Volume 2: The Lepton Collider (FCC-ee), Conceptual Design Report, edited by M. Benedikt *et al.*, CERN Accelerator Reports, CERN-ACC-2018-0057, submitted to *Eur. Phys. J. ST*, Geneva 2018.

[40] FCC Collaboration, Future Circular Collider Study Volume 3: The Hadron Collider (FCC-hh), Conceptual Design Report, edited by M. Benedikt *et al.*, CERN Accelerator Reports, CERN-ACC-2018-0058, submitted to *Eur. Phys. J. ST*, Geneva 2018.

[41] FCC Collaboration, Future Circular Collider Study Volume 4: The High Energy LHC (HE-LHC), Conceptual Design Report, edited by F. Zimmermann *et al.*, CERN Accelerator Reports, CERN-ACC-2018-0059, submitted to *Eur. Phys. J. ST*, Geneva 2018.

[42] The CEPC-SPPC Study Group, CEPC-SPPC Preliminary Conceptual Design Report, Volume I — Physics and Detector, IHEP-CEPC-DR-2015-01, March 2015.

[43] F. Su *et al.*, SPPC Parameter Choice and Lattice Design, Proceedings of IPAC2016, Busan, Korea, 2016, pp. 1400–1402.

[44] A.C. Canbay *et al.*, *Adv. High Energy Phys.* **2017**, 4021493 (2017).

[45] K. Hagiwara, D. Zeppenfeld, S. Komamiya, *Z. Phys. C* **29**, 115 (1985).

[46] U. Baur, M. Spira, P.M. Zerwas, *Phys. Rev. D* **42**, 815 (1990).

[47] F. Boudjema, A. Djouadi, *Phys. Lett. B* **240**, 485 (1990).

[48] F. Boudjema, A. Djouadi, J.L. Kneur, *Z. Phys. C* **57**, 425 (1993).

[49] A. Belyayev, N.D. Christensen, A. Pukhov, *Comput. Phys. Commun.* **184**, 1729 (2013).

[50] D. Stump *et al.*, *J. High Energy Phys.* **0310**, 046 (2003).

[51] O.J.P. Eboli, S.M. Lietti, P. Mathews, *Phys. Rev. D* **65**, 075003 (2002).